Title	Note: Readout of a micromechanical magnetometer for the ITER fusion reactor
Author(s)	Rimminen, Henry; Kyynäräinen, Jukka
Citation	Review of Scientific Instruments. AIP. Vol. 84 (2013) No: 5, 3 pages
Date	2013
URL	http://dx.doi.org/10.1063/1.4807718
Rights	Copyright (2013) American Institute of Physics. This article may be downloaded for personal use only. Any other use requires prior permission of the author and the American Institute of Physics.

AIP | Review of Scientific Instruments

Note: Readout of a micromechanical magnetometer for the ITER fusion reactor

H. Rimminen and J. Kyynäräinen

Citation: Rev. Sci. Instrum. **84**, 056110 (2013); doi: 10.1063/1.4807718
View online: http://dx.doi.org/10.1063/1.4807718
View Table of Contents: http://rsi.aip.org/resource/1/RSINAK/v84/i5
Published by the American Institute of Physics.

Note: Readout of a micromechanical magnetometer for the ITER fusion reactor

H. Rimminen[a] and J. Kyynäräinen
VTT Technical Research Centre of Finland, Tietotie 3, 02150 Espoo, Finland

(Received 13 March 2013; accepted 11 May 2013; published online 24 May 2013)

We present readout instrumentation for a MEMS magnetometer, placed 30 m away from the MEMS element. This is particularly useful when sensing is performed in high-radiation environment, where the semiconductors in the readout cannot survive. High bandwidth transimpedance amplifiers are used to cancel the cable capacitances of several nanofarads. A frequency doubling readout scheme is used for crosstalk elimination. Signal-to-noise ratio in the range of 60 dB was achieved and with sub-percent nonlinearity. The presented instrument is intended for the steady-state magnetic field measurements in the ITER fusion reactor. [http://dx.doi.org/10.1063/1.4807718]

In the ITER fusion reactor, steady-state plasma burning pulse lengths of an hour or more are anticipated. Conventional inductive coils, used in magnetic diagnostics for applications such as plasma position control, may suffer from drift during extended pulses because they require integration of the measured signal over time. Therefore, additional dc magnetometers are planned to be installed in ITER to improve measurement accuracy. Another purpose for these magnetometers is to map the absolute field created by the ferromagnetic inserts.[1]

The environment of the ITER fusion reactor will be harsh on sensors and electronics. The dc magnetometers will be installed on the outer surface of the vacuum vessel where temperatures up to 200 °C and high radiation doses, up to 15 MGy for both neutron and gamma radiation, are expected. A candidate for the sensor is VTT's MEMS magnetometer, originally developed for navigation applications.[2] This magnetometer consists of a vacuum encapsulated silicon torsion resonator, on top of which a molybdenum spiral coil has been deposited. Capacitive electrodes are formed on each side of the torsion plate for sensing or for electrostatic drive. The sensor is expected to have good radiation hardness since heavily doped silicon is used as metallic-like mechanical material, not as a semiconductor. Radiation hardened hall-effect magnetometers[1,3] offer another option for an ITER-like environment.

The sensors cannot be replaced during the 20-year lifetime of ITER, which prevents placing the readout in the vicinity of the sensors. The nearest location for the electronics is in the "port cell," at a distance of about 30 m from the sensor. In this paper, we present the performance of a realistic MEMS implementation for ITER in the laboratory.

There are two ways of operating the sensor as a magnetometer. First, if an ac current is fed to the coil in a magnetic field, the torsion plate starts to vibrate with an amplitude linearly dependent on the strength of the magnetic field. The sensitive axis of the sensor is in the plane of the torsion plate in such a way that the field is perpendicular to the torsion axis. The vibration amplitude can then be measured capacitively.[2] In this Note, we describe the second method in which the torsion plate is brought into vibration by electrostatic excitation and the sensed quantity is the voltage induced between the coil terminals in a magnetic field. The latter method was selected for its simpler design and fewer cables required. In both readout schemes, operating the sensor at the mechanical resonance frequency boosts the sensitivity by the mechanical Q value.

The mechanical resonance frequency of the sensor used in the experiments is 31 kHz and the Q factor is approximately 1000. The spiral coil has $N = 45$ turns with exterior dimensions of 1×1 mm^2. Resistance of the coil is 30 kΩ and electrode capacitance is 1.2 pF. Parasitic capacitance of the 30 m twisted pair cable is 3.9 nF from each lead to ground and the MEMS coil resistance is 30 kΩ. If a simple voltage amplifier was used, the time constant would cause 32 dB attenuation. In this Note, we employ high-bandwidth transimpedance amplifiers (TIA) to cancel the parasitic capacitance. In theory, a TIA keeps the signal wire potential at 0 V, so there is no displacement current to the cable shield. The capacitance limits the achievable current-to-voltage (I-V) gain at the desired frequency. High bandwidth of the amplifier is the only antidote.

A drawback of using TIAs is noise peaking. It is caused by increase of voltage noise gain as a function of frequency.[4,5] The noise gain is set by the ratio of the cable reactance and feedback impedance. In some applications, such as photo diode detection, the noise peak can be removed by a cascaded TIA. The parallel capacitance is isolated from the input of the TIA with a bipolar junction transistor and with additional circuitry.[4] In our simulations and experiments we failed to get the cascaded TIA operational, which might be due to parasitic capacitance that is a decade higher than that of photo diodes. Thus, we ended up using a traditional TIA and simply avoiding the noise peak. With proper selection of the amplifier, the I-V gain and the I-V bandwidth, the measurement signal can be set in the "noise valley" between the 1/f noise corner and the TIA noise peak.

The OPA659 operational amplifier from Texas Instruments was used as the TIA. It has low current noise (1.8 fA/$\sqrt{}$Hz) due to its JFET input and relatively high unity-gain bandwidth (650 MHz). I-V gain was set to 100 kΩ, and I-V

[a]E-mail: henry.rimminen@vtt.fi

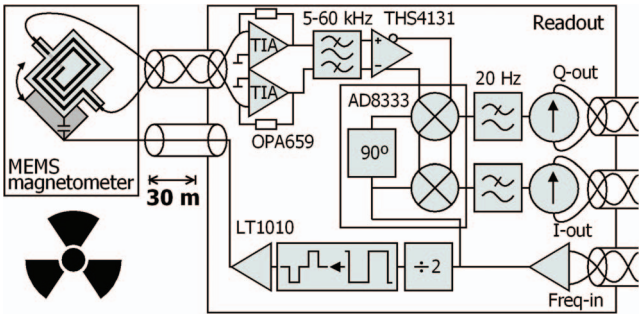

FIG. 1. Block diagram of the implemented readout instrument. It will interface a control unit placed 100 m away (not shown).

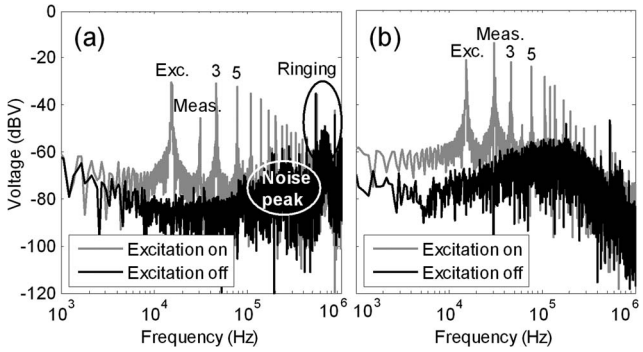

FIG. 2. Discrete Fourier transforms with 30 m cables when excitation is on and off. (a) After TIA and (b) after the bandpass filter and the differential gain stage.

bandwidth was set to 100 kHz. These, together with our cable capacitance, cause noise peaking at 300 kHz. Measurement frequency is 31 kHz.

Crosstalk from the excitation source creates offset in the measured signal, which limits the dynamic range. Crosstalk also makes the resonator's phase-behavior ambiguous, which makes it difficult to implement resonance tracking control for the excitation frequency. A very useful crosstalk elimination scheme has been presented by Rödjegård and Andersson in 2005.[6] They utilize the fact that electrostatically actuated MEMS doubles the excitation frequency inherently when no dc bias is used. This is because the electrostatic force is polarity-independent. Thus, the crosstalk is at a different frequency to the measurement signal and can be easily filtered out. Phase response is then unambiguous and resonance tracking is simple.

The excitation waveform was also adopted from Rödjegård and Andersson. They proposed a semi-digital excitation waveform, which is easily generated from a digital input and contains no second harmonic.[6] The lack of second harmonic is essential for the crosstalk elimination. The odd harmonics are prominent, but do not degrade the overall performance. Suitable excitation amplitude was 24 V peak-to-peak, which was sought experimentally.

The complete implementation is shown in Figure 1. The TIAs cancel the capacitances of the shielded twisted pair leads separately. The bandpass filter and the differential gain stage (30 dB) are implemented with two low-noise differential operational amplifiers (THS4131). The pass-band is wide (5–60 kHz) so its phase response is flat, but the noise peak of the TIA is attenuated. The AD8333 was selected as the mixer for its best-in-class phase accuracy and balance between the channels. The 20-Hz low-pass filters after the mixer reject the crosstalk and its harmonics. The LT1010 power buffer is used to drive the excitation for its excellent tolerance for capacitive loads. Note that the frequency is divided by two before the semi-digital generator and driver, since the MEMS doubles it.

A control unit is located 100 m away from the readout (not shown in Figure 1). This is why the detected signals (I-out, Q-out) are sent forward with 4–20 mA current loops. The frequency is fed remotely from the control unit with RS–485 physical layer to ensure maximal tolerance for interference. The use of a voltage controlled oscillator in the readout instrument was discarded because of large phase noise and susceptibility to interference. The control unit will handle temperature compensation of both the MEMS element and the readout instrument using thermocouples. Calibration of the MEMS element will be maintained with an external coil.

All of the following results have been obtained with 30 m cables. Figure 2 shows discrete Fourier transforms with a 0.28-T flux density, created by a permanent magnet. Part (a) is after the TIA and part (b) is after the bandpass filter and the differential gain stage. In Figure 2(a), one can see the main component of the crosstalk at 15.5 kHz (denoted by Exc.) and its odd harmonics (first two denoted by 3 and 5). The even harmonics are virtually absent. At a double frequency (31 kHz), one can see the measurement signal (denoted by Meas.). It is located in the "noise valley" between the 1/f noise and noise peak of the TIA. Although the OPA659 was the most stable amplifier found, some ringing is still visible around 600 kHz. Due to its low amplitude and high frequency, it can be ignored.

By comparing Figures 2(a) and 2(b), one can see how the measurement signal is amplified more than the crosstalk and its harmonics. This is because the differential gain stage rejects common mode signals. The crosstalk is mostly common mode since it couples capacitively from the driving electrode to both of the coil terminals. The reason why better common mode rejection is not achieved is that the spiral MEMS coil is asymmetric and the crosstalk also has a differential component.

Figure 3 shows the measured output of the readout instrument with a 0.28-T flux density. Sweep time was 5 s and

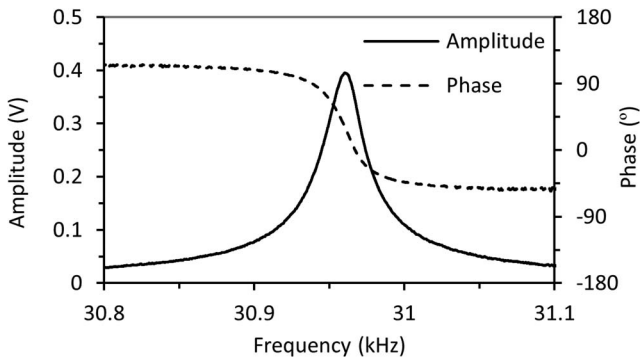

FIG. 3. Measured output of the readout as a function of frequency with 30 m cables.

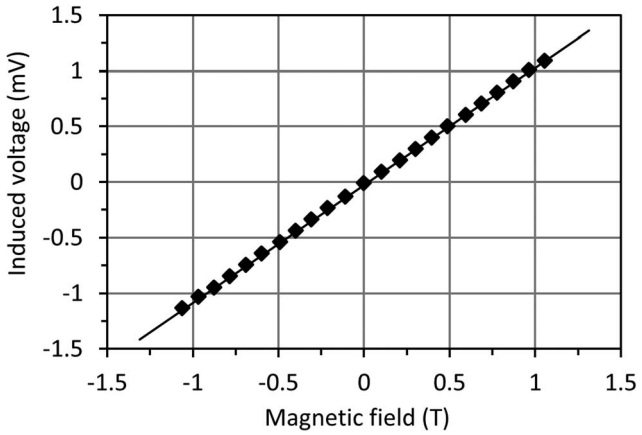

FIG. 4. Amplitude of the induced voltage as a function of the flux density with 30 m cables.

sweep width was 300 Hz. Amplitude and phase has been calculated from I- and Q-channel voltages after removing a 13–mV static offset. The phase slope is unambiguous and the amplitude peak is symmetric. We conclude that the crosstalk elimination works as predicted.[6] The peak voltage is 395 mV. At 0.28 T the in-resonance output noise voltage is 0.455 mV (RMS, 20 s, 1–20 Hz, HP 3458A).

Thus, the signal-to-noise ratio is 59 dB and the noise limited resolution is 0.3 mT.

Figure 4 shows the induced voltage as a function of the flux density between ±1.1 T. The voltage has been reduced to the MEMS coil terminals taking into account the total gain. The sensitivity is 1.1 mV/T, which generates 37 nA/T. The maximum nonlinearity error is 0.4% of full scale. The error is partly due to calibration of the test magnet.

Special thanks belong to Lawrence Jones, who sourced Ref. 6 and suggested sensing of the coil voltage instead of capacitive readout. This work was partly supported by Fusion for Energy Grant No. F4E-GRT-156 and by TEKES, the Finnish Funding Agency for Technology and Innovation. The views expressed in this publication are the sole responsibility of the authors and do not necessarily reflect the views of the Fusion for Energy and the ITER Organization. Neither Fusion for Energy nor any person acting on behalf of Fusion for Energy is responsible for the use, which might be made of the information in this publication.

[1]R. Chavan, G. Chitarin, R. S. Delogu, A. Encheva, A. Gallo, E. R. Hodgson, L. C. Ingesson, A. Le-Luyer, J. B. Lister, Ph. Moreau, J.-M. Moret, S. Peruzzo, J. Roméro, D. S. Testa, M. Toussaint, G. Vayakis, and R. Vila, Fusion Eng. Des. **84**, 295 (2009).
[2]J. Kyynäräinen, J. Saarilahti, H. Kattelus, A. Kärkkäinen, T. Meinander, A. Oja, P. Pekko, H. Seppä, M. Suhonen, H. Kuisma, S. Ruotsalainen, and M. Tilli, Sens. Actuators, A **142**, 561 (2008).
[3]I. Bolshakova, I. Duran, R. Holyaka, K. Kovarik, C. Leroy, A. Marusenkov, J. Sentkerestiová, J. Stockel, L. Viererbl, and V. Yerashok, Orlinski, in *Proceedings of the 36th EPS Conference on Plasma Physics Sofia, 29 June–3 July 2009* (European Physical Society, Mulhouse, France, 2009), Vol. 33E, P-4.169.
[4]P. C. D. Hobbs, Opt. Photonics News **12**, 44 (2001).
[5]S. Lányi, Meas. Sci. Technol. **12**, 1456 (2001).
[6]H. Rödjegård and G. I. Andersson, Sens. Actuators, A **121**, 72 (2005).